Available online at www.sciencedirect.com
ScienceDirect
Catalysis Today 129 (2007) 355–364
CATALYSIS TODAY
www.elsevier.com/locate/cattod

Production of hydrogen by steam reforming of glycerin over alumina-supported metal catalysts

Sushil Adhikari, Sandun Fernando *, Agus Haryanto

Department of Agricultural and Biological Engineering, Mississippi State University, Mississippi State, MS 39762, USA

Available online 29 September 2007

Abstract

Use of biodiesel and its production are expected to grow steadily in the future. With the increase in production of biodiesel, there would be a glut of glycerin in the world market. Glycerin is a potential feedstock for hydrogen production because one mol of glycerin can produce up to four mols of hydrogen. However, less attention has been given for the production of hydrogen from glycerin. The objective of this study is to develop, test and characterize promising catalysts for hydrogen generation from steam reforming of glycerin. Fourteen catalysts were prepared on ceramic foam monoliths (92% Al_2O_3, and 8% SiO_2) by the incipient wetness technique. This paper discusses the effect of these catalysts on hydrogen selectivity and glycerin conversion in temperatures ranging from 600 to 900 °C. The effect of glycerin to water ratio, metal loading, and the feed flow rate (space velocity) was analyzed for the two best performing catalysts. Under the reaction conditions investigated in this study, Ni/Al_2O_3 and $Rh/CeO_2/Al_2O_3$ were found as the best performing catalysts in terms of hydrogen selectivity and glycerin conversion. It was found that with the increase in water to glycerin molar ratio, hydrogen selectivity and glycerin conversion increased. About 80% of hydrogen selectivity was obtained with Ni/Al_2O_3, whereas the selectivity was 71% with $Rh/CeO_2/Al_2O_3$ at 9:1 water to glycerin molar ratio, 900 °C temperature, and 0.15 ml/min feed flow rate (15300 GHSV). Although increase in metal loading increased glycerin conversion for both catalysts, hydrogen selectivity remained relatively unaffected. At 3.5 wt% of metal loading, the glycerin conversion was about 94% in both the catalysts.

Keywords: Glycerin; Conversion; Selectivity; Hydrogen

1. Introduction

At present, almost 95% of the hydrogen (H_2) is being produced from fossil fuel-based feedstocks [1] and most is used as a chemical ingredient in petrochemical, metallurgical, food, and electronics processing industries [2]. Demand for H_2, the simplest and most abundant element, is growing due to the technological advancements in fuel cell industry [3]. If the present scenario in the production of H_2 exists, the more carbon will be converted into carbon dioxide (CO_2), a major greenhouse gas, and released into the atmosphere leading to the global climate change. The effect of climate change is immense, such as rise in sea level and increase in the earth's temperature. Furthermore, recent studies have shown that climate change has led to genetic changes in populations of animals such as birds, squirrels, and mosquitoes [4]. Renewable resources-based technologies for H_2 production are seen as viable options for the future due to the carbon neutral nature with lesser effects on global climate. In biomass technologies, the production of H_2 from ethanol has been studied widely [5–8]. However, ethanol has been successfully blended with the gasoline up to 85% and has been used in gasoline engines in many countries to curb the emissions from transport sector and reduce dependency on petroleum products [9]. Accordingly, it would be prudent to explore other resources, which cannot be used easily in the existing infrastructure, rather than producing hydrogen from ethanol, currently used as a substitute of gasoline.

Biodiesel, a renewable fuel targeted for compression ignition engines, is widely being implemented around the world. Its production is expected to grow rapidly in the future. For example, the production of biodiesel in the United States was about 25 million gal in 2004 and increased by threefolds, 75 million gal in 2005 [10,11]. In converting vegetable oils into biodiesel, about 10 wt% of glycerin ($C_3H_8O_3$) is produced as a byproduct. With increase in production of biodiesel, a glut of glycerin is expected in the world market and therefore, it is

* Corresponding author. Tel.: +1 662 325 3282; fax: +1 662 325 3853.
E-mail address: sf99@abe.msstate.edu (S. Fernando).

0920-5861/$ – see front matter
doi:10.1016/j.cattod.2006.09.038

essential to find useful applications for glycerin. One possibility of using glycerin is as a renewable source to produce H_2. Compared to ethanol, glycerin has more number of moles of H_2 in its chemical structure and would be a logical substrate to produce H_2.

To date, only a handful of studies have attempted glycerin reforming [12–14]. Dumesic and co-workers [14–17] produced H_2 from biomass derived oxygenated hydrocarbons including glycerin in an aqueous phase reforming process. Although catalyst performance was stable for a week, high pressure and slow reaction rates have hindered its use as a commercially viable process. On the other hand, the steam reforming process can be carried out at atmospheric pressure. Steam reforming is the most energy efficient technology available, and it is the most cost-effective [18]. It is strongly endothermic, and ideally, it must be carried out at high temperatures, low pressure, and high steam to glycerin ratio to achieve higher conversion [19]. Czernik et al. [13] reported steam reforming of crude glycerin using a commercial nickel-based naphtha reforming catalyst (C11-NK); however, detailed results were not reported. Recently, Suzuki and co-workers [12] reported the performance of the catalysts loaded with Groups 8–10 metals mainly in La_2O_3 supports for glycerin reforming at 500 and 600 °C, and steam to carbon ratio 3.3.

The steam reforming reaction of glycerin proceeds according to the following equations [12]:

Steam reforming of glycerin:

$$C_3H_8O_3 \xrightarrow{H_2O} 3CO + 4H_2 \quad (1)$$

Water-gas shift reaction:

$$CO + H_2O \Leftrightarrow CO_2 + H_2 \quad (2)$$

Methanation reaction:

$$CO + 3H_2 \rightarrow CH_4 + H_2O \quad (3)$$

The overall reaction at ideal conditions can be given as follows:

$$C_3H_8O_3 + 3H_2O \rightarrow 3CO_2 + 7H_2 \ (\Delta H^0_{298} = +346.4\,\text{kJ/mol}) \quad (4)$$

Ni [20–24] and noble metal-based [5,25,26] catalysts were widely used in the ethanol steam reforming and detailed reviews on the catalysts can be found elsewhere [27,28]. It is assumed that the active catalysts for ethanol steam reforming are also active in glycerin steam reforming. Therefore, Ni and noble metal-based catalysts were attempted for H_2 production from glycerin steam reforming in this study. The idea of choosing Ni catalysts with other noble metal-based catalysts was that, Ni has been used as a steam reforming catalyst for a long time and would help to compare the performance of a relatively cheaper catalyst, such as Ni, with noble metal-based catalysts. In this study, we have investigated the performance of Ni and platinum group metal-based catalysts on Al_2O_3 and CeO_2/Al_2O_3 supports. A total of 14 catalysts were prepared and their performance was analyzed at four different temperatures between 900 and 600 °C. Based on the results, two best performing catalysts, in terms of H_2 selectivity and high glycerin conversion, were selected for a detailed study. The effect of water to glycerin molar ratios (WGR), metal loading, and the feed flow rate (FFR) or gas hourly space velocity (GHSV) were analyzed for the two best performing catalysts. It is true that the glycerin produced from biodiesel plants is not pure, but we have used pure glycerin in this study to avoid complexity associated with interpretation of results.

2. Experimental

2.1. Catalyst preparation

Metals used for the catalysts preparation were as follows: (i) Rh; (ii) Pt; (iii) Pd; (iv) Ir; (v) Ru; and (vi) Ni. Catalysts were prepared by the incipient wetness technique using nitrate and chlorate precursors. All catalysts were prepared on alumina (92%) ceramic foam monoliths containing 8% silica from Vesuvius Hi Tech Ceramics (Champaign, IL). The monoliths had nominal surface area of ~1 m^2/g with a void fraction of about 0.8. Industrial processes typically require catalysts deposited in structural supports, such as pellets or monoliths to minimize the pressure drop in the reactor [29]. Therefore, monoliths supports were used in this study. Similarly, CeO_2 was loaded on the monolith to prepare Metal/CeO_2/Al_2O_3 catalysts. The reason behind choosing CeO_2 is that it often exhibits strong resistance to coke deposition based on oxygen storage-release capacity [25,30]. Altogether 14 catalysts (Al_2O_3; Rh/Al_2O_3; Pt/Al_2O_3; Pd/Al_2O_3; Ir/Al_2O_3; Ru/Al_2O_3; Ni/Al_2O_3; Ce/Al_2O_3; $Rh/Ce/Al_2O_3$; $Pt/Ce/Al_2O_3$; $Pd/Ce/Al_2O_3$; $Ir/Ce/Al_2O_3$; $Ru/Ce/Al_2O_3$; and $Ni/Ce/Al_2O_3$) were prepared for the experiments. $Rh(NO_3)_3$, H_2PtCl_6, $Pd(NO_3)_2$, H_2Cl_6Ir, $HN_4O_{10}Ru$, $Ni(NO_3)_2{\cdot}6H_2O$, and $Ce(NO_3)_3{\cdot}6H_2O$ were used for the catalysts preparation and purchased from Sigma–Aldrich (St. Louis, MO). All the monoliths were loaded with metal 2.5 wt% of the monoliths unless otherwise stated. Monoliths were dried at 125 °C for 1 h and calcined at 700 °C for 5 h in air. In case that the amount of metal solution was too much to be loaded at once, and the loading was repeated after drying for around an hour at 125 °C until the complete metal loading was achieved. The monoliths were left overnight in the furnace for cooling and reweighed to confirm the required metal loading based on the mass of monoliths. It should be noted that although we present the catalyst in the form "Metal/Al_2O_3", most likely the metals were in oxide forms because catalysts were not reduced prior, during or subsequent to test runs. This will be confirmed by the XRD analysis that will be presented later.

2.2. Catalyst performance testing

Fig. 1 shows the schematic of glycerin steam reforming process. All experiments were carried out in a tubular furnace that could reach temperatures up to 1100 °C. The experiments

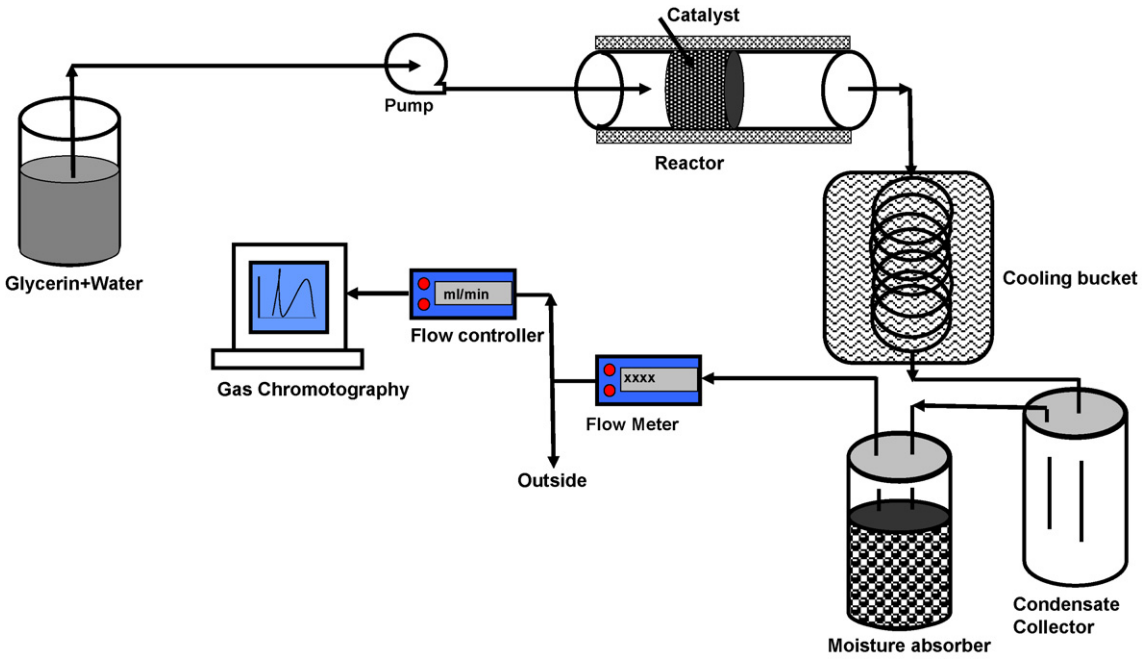

Fig. 1. Schematic of glycerin steam reforming setup.

were carried out at a constant flow rate of 0.5 ml/min unless otherwise mentioned and at four furnace temperatures from 600 to 900 °C. Glycerin and water were mixed in a separate container at particular WGR, and the mixture was supplied into the reactor using a HPLC pump (LC-20AT, Shimadzu Scientific Instrument, Columbia, MD). As depicted in Fig. 1, the coated monoliths were placed in the middle of the tubular reactor. Monoliths were held at the center of the reactor with the help of alumina cloths. The reactor was made of alumina (99.8%) tube with 19 mm inner diameter and was purchased from McDanel Advanced Ceramic Technologies LLC (Beaver Falls, PA). Molar concentration of glycerin and water was 1:6 and kept constant throughout the experiment unless otherwise stated. Gas stream from the reactor was cooled using crushed ice and water. The unreacted water and other liquids formed during the reaction were collected. The outlet gas was sent through a moisture trap before purging to the gas chromatograph (GC6890, Agilent Technologies Incorporated, Palo Alto,

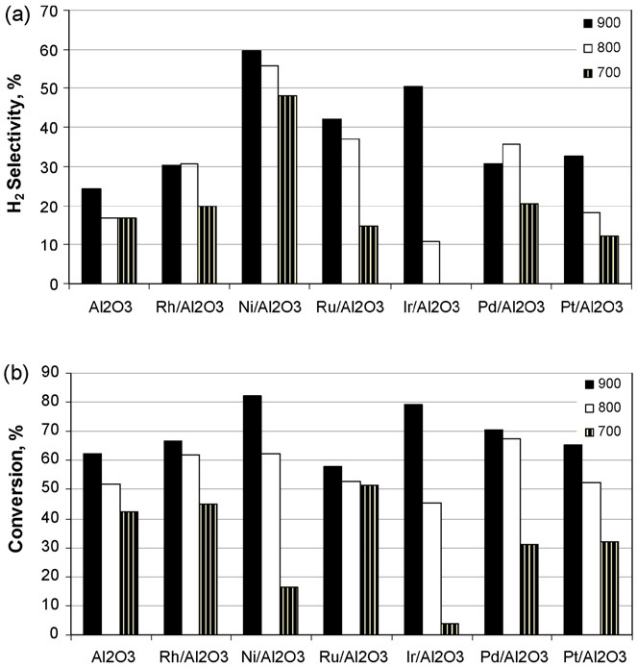

Fig. 2. (a) H_2 selectivity and (b) glycerin conversion at selected temperatures over Al_2O_3-supported catalysts. Reaction conditions: WGR = 6:1, FFR: 0.5 ml/min (GHSV = 51000 h^{-1}), data collected after 1 h of operation.

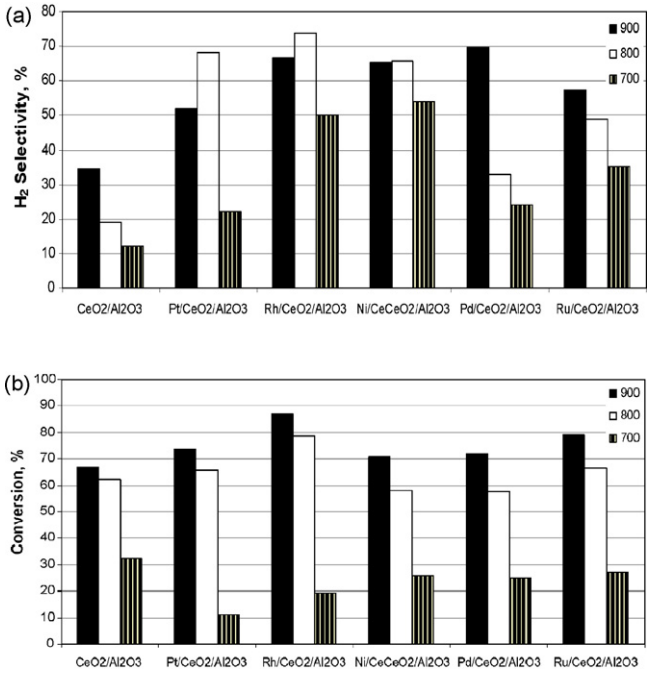

Fig. 3. (a) H_2 selectivity and (b) glycerin conversion at selected temperatures over CeO_2/Al_2O_3-supported catalysts. Reaction conditions: WGR = 6:1, FFR: 0.5 ml/min (GHSV = 51000 h^{-1}), data collected after 1 h of operation.

CA). H_2 content in the outlet was analyzed by a thermal conductivity detector with Molecular Sieve column. The concentrations of carbon monoxide (CO), methane (CH_4), and CO_2 were analyzed by a flame ionization detector with HP-Plot Q column. Only four gases including H_2 were analyzed in this study.

The performance of the catalyst is presented in terms of H_2, CO, CH_4, and CO_2 selectivity, and glycerin conversion. Selectivity and the glycerin conversion were calculated based on the following equations:

$$\%\,\mathrm{H_2\ selectivity} = \frac{\mathrm{H_2\ moles\ produced}}{\mathrm{C\ atoms\ produced\ in\ gas\ phase}} \times \frac{1}{\mathrm{RR}} \times 100 \quad (5)$$

where RR is H_2/CO_2 reforming ratio [14] and it is 7/3 in the case of glycerin steam reforming process (see Eq. (4)).

$$\%\,\mathrm{Selectivity\ of}\ i = \frac{\mathrm{C\ atoms\ in\ species}\ i}{\mathrm{C\ atoms\ produced\ in\ gas\ phase}} \times 100 \quad (6)$$

where species i = CO, CO_2, and CH_4.

$$\%\,\mathrm{Conversion} = \frac{\mathrm{C\ atoms\ in\ gas\ products}}{\mathrm{Total\ C\ atoms\ in\ the\ feedstock}} \times 100 \quad (7)$$

There could be some error while calculating glycerin conversion based on the carbon balance from gas products because we analyzed only three carbon containing gases (CO, CO_2, and CH_4) and some inconspicuous unidentified peaks were noticed during the gas analysis. Perhaps the unidentified peaks could be C_2-hydrocarbons (ethane and ethylene) [31]. Also, the condensate collected after the reaction was not analyzed although there could be other organic compounds, such as ethylene glycol, methanol, hydroxypropane and ethanol, besides unconverted glycerin [31].

2.3. Catalyst characterization

Two best performing catalysts were sent for X-ray diffraction (XRD) analysis. Also, scanning electron microscope (SEM) images were taken to observe the dispersion of the

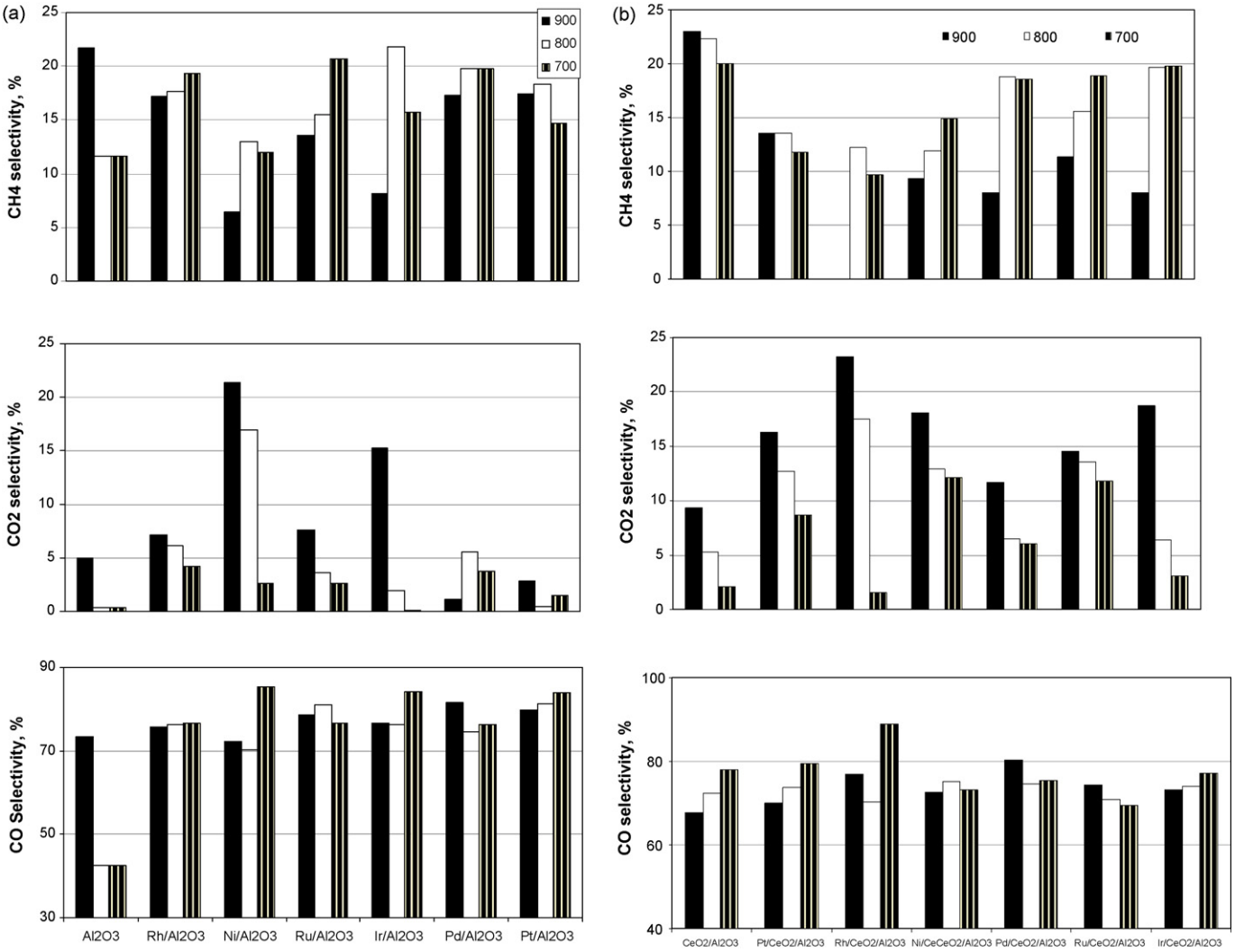

Fig. 4. CO, CO_2, and CH_4 selectivity over (a) Al_2O_3, and (b) CeO_2/Al_2O_3-supported catalysts. Reaction conditions: WGR = 6:1, FFR: 0.5 ml/min (GHSV = 51000 h^{-1}), data collected after 1 h of operation.

metals on the supports. Energy dispersive spectroscopy (EDS) mappings were taken from the two best catalysts.

3. Results and discussion

3.1. Effect of metal

Fig. 2 depicts the H_2 selectivity and the glycerin conversion for the selected catalysts over Al_2O_3 supports. As can be seen from Fig. 2(a), Ni/Al_2O_3-supported catalyst showed the highest selectivity for H_2 compared to other platinum group metal-based catalysts at all temperatures investigated in this study. The maximum H_2 selectivity with Ni/Al_2O_3 was 60%, 56%, and 48% at 900, 800, and 700 °C, respectively. Catalytic conversion of glycerin to H_2, CO_2, and CO involves the preferential cleavage of C–C bonds as opposed to C–O bonds [14]. It is generally accepted that nickel promotes C–C rupture [32]. Although Pt-based catalysts are also active and selective for this process, the performance of Pt/Al_2O_3 was found to be lower compared to Ni/Al_2O_3 and Ru/Al_2O_3 in the present study. The H_2 selectivity for the reaction at 900 °C was in the order: Ni > Ir > Ru > Pt > Rh, Pd.

Since the steam reforming of glycerin is a highly endothermic reaction, high temperature favors glycerin conversion. As can be seen from Fig. 2(b), conversion of glycerin increased with the increase in temperature and reached a maximum at 900 °C for all the catalysts. The maximum conversion was obtained with Ni/Al_2O_3 and was 82% at 900 °C. As the temperature decreased, the conversion decreased and at 600 °C (not shown here) the conversion was less than 5% in all catalysts except for Ni/Al_2O_3, which was around 10%. Although Ni/Al_2O_3 showed a higher H_2 selectivity and glycerin conversion (at 900 °C) compared to that of Al_2O_3-supported platinum metal-based catalysts, it lost structural integrity at lower temperatures. Similar behavior of Ni/Al_2O_3 was also observed in ethanol steam reforming and the problem was resolved by using La_2O_3 [22,33]. The advantage of Ni-based catalyst is that it is much cheaper compared to the noble metal-based catalysts. Unlike in H_2 selectivity, where Ni/Al_2O_3 showed the best selectivity at all temperatures, Ni/Al_2O_3 (82%), Pd/Al_2O_3 (67%), and Ru/Al_2O_3 (51%) showed the highest conversions at 900, 800, and 700 °C, respectively. The glycerin conversion for the reaction at 900 °C was in the order: Ni > Ir > Pd > Rh > Pt > Ru.

It is widely known that the catalyst support plays important role in the conversion process. Fig. 3 depicts the selectivity and the conversion of CeO_2/Al_2O_3-supported catalysts. $Pd/CeO_2/Al_2O_3$ showed the maximum H_2 selectivity (70%) at 900 °C, whereas $Rh/CeO_2/Al_2O_3$ showed the highest H_2 selectivity (74%) at 800 °C. At 700 °C, $Ni/CeO_2/Al_2O_3$ showed the maximum selectivity (54%) towards H_2. With the addition of CeO_2, all the catalysts showed the higher H_2 selectivity than with Al_2O_3-supported catalysts. However, glycerin conversion showed mix results. At 900 and 800 °C, all the catalysts showed higher conversion than only with Al_2O_3 supports, whereas at 700 °C, especially Pt, Rh and Ru-supported catalysts showed

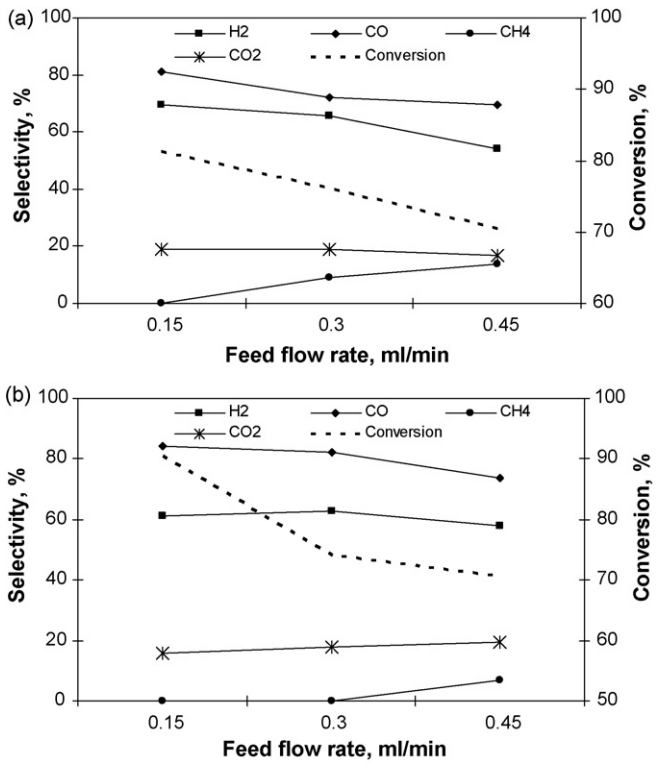

Fig. 5. Selectivity and glycerin conversion over (a) Ni/Al_2O_3, and/(b) $Rh/CeO_2/Al_2O_3$ at selected flow rates. Reaction conditions: reaction temperature = 900 °C, WGR = 6:1, data collected after 1 h of operation.

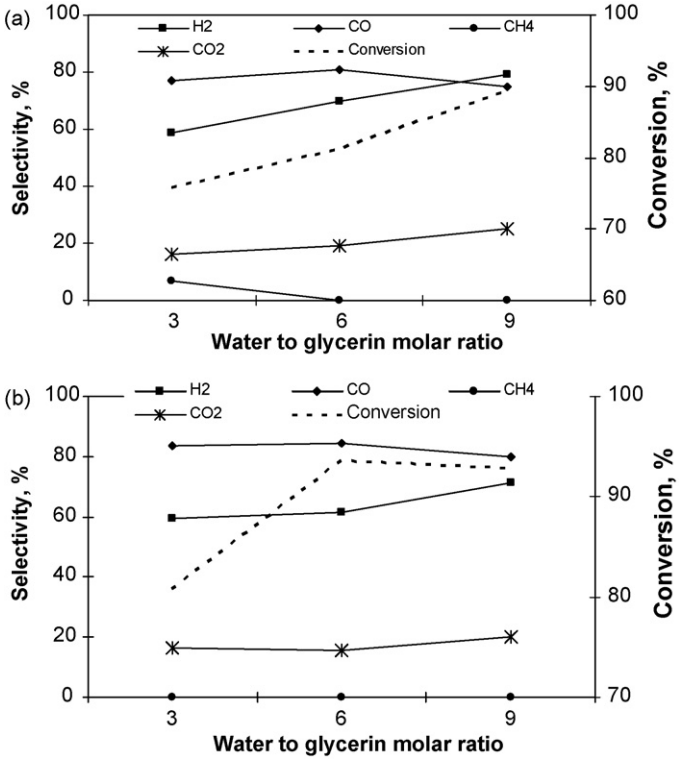

Fig. 6. Selectivity and glycerin conversion over (a) Ni/Al_2O_3, and (b) $Rh/CeO_2/Al_2O_3$ at selected glycerin to water molar ratios. Reaction conditions: reaction temperature = 900 °C, FFR = 0.15 ml/min (GHSV = 15,300 h^{-1}), data collected after 1 h of operation.

lower conversions than that of CeO_2/Al_2O_3 alone. The highest conversion was about 87% and 77% at 900 and 800 °C, respectively with $Rh/CeO_2/Al_2O_3$. Overall, the addition of CeO_2 showed a positive effect in both H_2 selectivity and the conversion for most of the catalysts. Perhaps, this could be due to the promoting effect of CeO_2 and more importantly, CeO_2 itself participating in the steam reforming process (Fig. 3).

As can be seen from Fig. 4, all the catalysts were highly selective towards CO, whereas CO_2 selectivity was found to be lower in all the catalysts. This can be attributed to the primary reaction in glycerin steam reforming as per Eq. (1) and water gas shift reaction is the secondary reaction. CO selectivity was always greater than 70% with all the catalysts as shown in Fig. 4. On the other hand, CO_2 selectivity was never greater than 25%. Ni/Al_2O_3 and $Rh/CeO_2/Al_2O_3$ showed the maximum CO_2 selectivity. In the case of CH_4 selectivity, it increased with decreased reaction temperatures in most of the catalysts, which is thermodynamically possible [34]. Formation of CH_4 was almost completely inhibited with $Rh/CeO_2/Al_2O_3$ at 900 °C. At high temperatures, CH_4 steam reforming process is possible [35] and this could be attributed to the decrease in CH_4 selectivity at high temperature (Eq. (8)). Based on the H_2 selectivity and glycerin conversion, Ni/Al_2O_3 and $Rh/CeO_2/Al_2O_3$ were the best performing catalysts in this study. It should be noted that two best catalysts selected from 14 catalysts in our study are valid only on the given experimental conditions. It might be the case that there could be other catalysts which could perform better than the two best catalysts selected in this study in other experimental conditions.

$$CH_4 + H_2O \rightarrow CO + H_2 \quad (8)$$

3.2. Effect of feed flow rate

Three different flow rates (0.15, 0.3, and 0.45 ml/min) were used to investigate the effect of the FFR in terms of glycerin conversion and the H_2 selectivity for Ni/Al_2O_3 and $Rh/CeO_2/Al_2O_3$ catalysts. The H_2 selectivity and glycerin conversion increased with a decrease in flow rate (Fig. 5). With Ni/Al_2O_3, 81% and 70% conversion and H_2 selectivity, respectively were obtained at 0.15 ml/min. With the increase in FFR from 0.15 to 0.3 ml/min, the conversion and H_2 selectivity dropped to 76% and 66%, respectively. Further increase in FFR to 0.45 ml/min, the conversion and H_2 selectivity dropped to 70% and 54%, respectively. Similarly, with $Rh/CeO_2/Al_2O_3$ glycerin conversion and H_2 selectivity were 90% and 61%, respectively at 0.15 ml/min FFR. With increase in FFR from 0.15 to 0.3 ml/min, glycerin conversion dropped to 74%, whereas there was very small increase (63%) in H_2 selectivity. Likewise, increase in FFR to 0.45 ml/min dropped glycerin conversion to 70% and H_2 selectivity to 58%. It can be noticed that there are some inconsistencies between the results of glycerin conversion obtained with both catalysts at 0.5 and 0.45 ml/min (Figs. 2b and 5a for Ni/Al_2O_3, Figs. 3b and 5b for $Rh/CeO_2/Al_2O_3$). This could be attributed to the following reason: different samples of the catalyst were used for the test conditions. The weight of monoliths was not uniform although the metal loading was 2.5 wt% of the monoliths. Higher glycerin conversion could

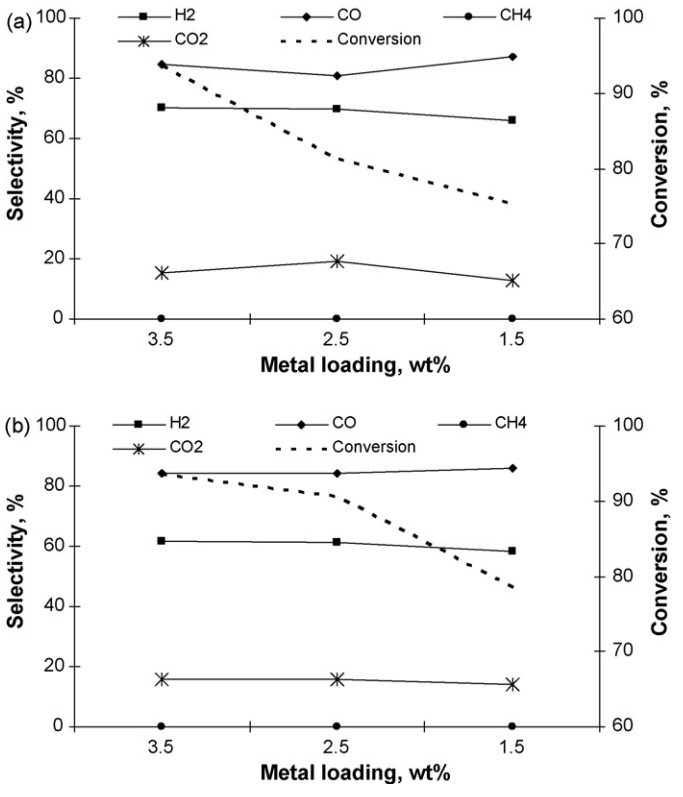

Fig. 7. Selectivity and glycerin conversion over (a) Ni/Al_2O_3, and (b) $Rh/CeO_2/Al_2O_3$ at different metal loading. Reaction conditions: reaction temperature = 900 °C, FFR = 0.15 ml/min, WGR = 6, data collected after 1 h of operation.

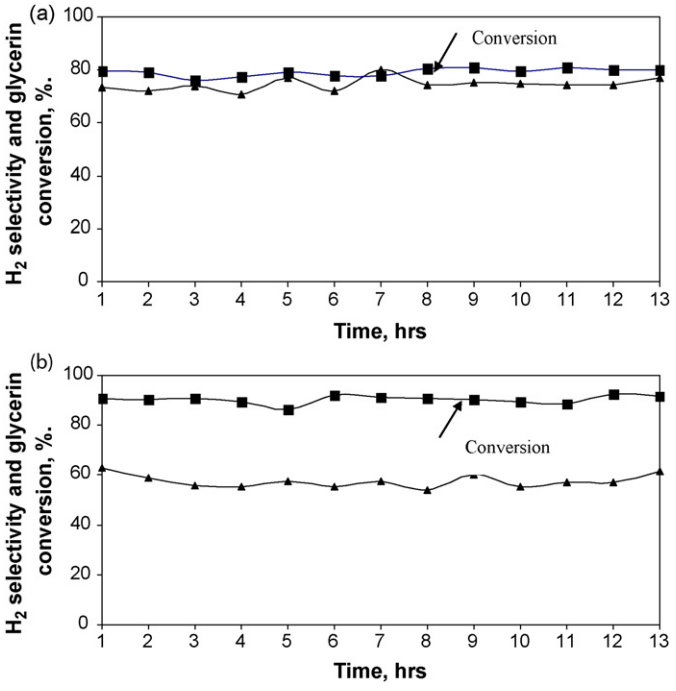

Fig. 8. Selectivity and glycerin conversion over (a) Ni/Al_2O_3, and (b) $Rh/CeO_2/Al_2O_3$ for 13 h. Reaction conditions: reaction temperature = 900 °C, FFR = 0.15 ml/min, WGR = 6.

results due to the higher metal loading in Figs. 2b and 3b for Ni/Al_2O_3 and Rh/CeO_2/Al_2O_3, respectively compared to Fig. 5a (Ni/Al_2O_3) and 5b (Rh/CeO_2/Al_2O_3).

As can be seen from Fig. 5, at 0.15 ml/min no CH_4 was observed in the gas streams with both catalysts, Ni/Al_2O_3 and Rh/CeO_2/Al_2O_3. However, with the increase in the flow rate, selectivity towards CH_4 increased under the given conditions. At FFR of 0.45 ml/min, CH_4 selectivity was 13% and 6% with Ni/Al_2O_3 and Rh/CeO_2/Al_2O_3, respectively. Obviously, the formation of CH_4 in the glycerin reforming is not desirable

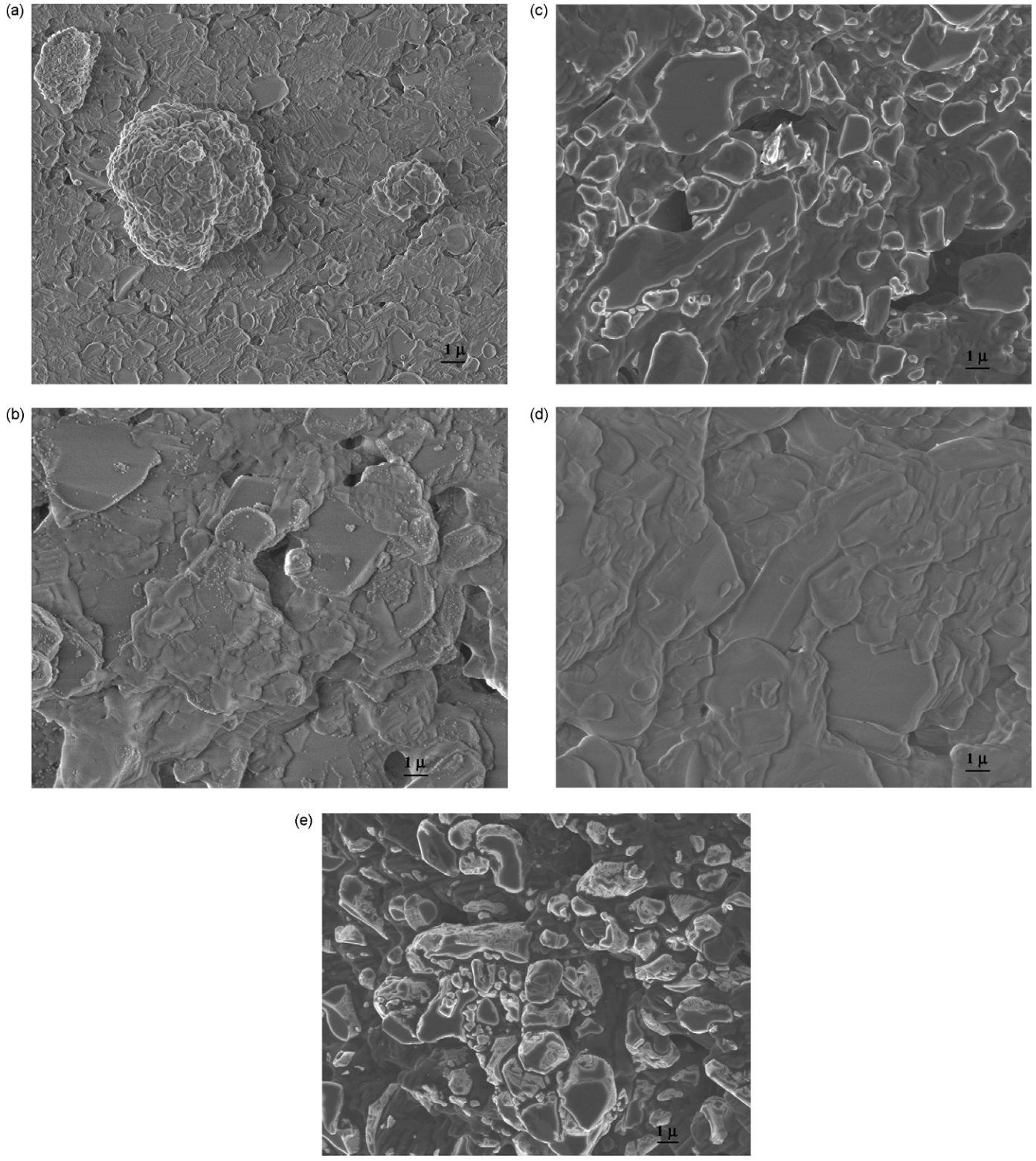

Fig. 9. SEM images of: (a) blank Al_2O_3; (b) Ni/Al_2O_3; (c) Rh/Al_2O_3; (d) CeO_2/Al_2O_3; and (e) Rh/CeO_2/Al_2O_3 before the reaction.

because it reduces the selectivity towards H_2. At high glycerin conversion, the selectivity towards CO is higher than CO_2 and CO selectivity reduced with decrease in conversion. As mentioned earlier, this can be attributed to occurrence of the primary reaction in glycerin reforming as dictated by Eq. (1). Ratio of H_2/CO (not shown here) varied from 1.6 to 2.0, which is slightly higher than given by Eq. (1). This behavior suggests that water gas shift reaction (Eq. (2)) is the secondary reaction which further converts CO and water to H_2 and CO_2 and therefore increase the ratio of H_2/CO higher than as given by Eq. (1) (1.33). It was found that the increase in FFR decreased glycerin conversion and H_2 selectivity with both catalysts. In the case of Ni/Al_2O_3, increase in FFR decreased glycerin conversion steadily, whereas it was not the same for $Rh/CeO_2/Al_2O_3$, especially between 0.3 and 0.45 ml/min (see Fig. 5).

3.3. Effect of water to glycerin ratio

Fig. 6 shows the effect of the WGRs in H_2, CO, CO_2, and CH_4 selectivity and the glycerin conversion. With the increase in WGRs, the glycerin conversion increased monotonously in case of Ni/Al_2O_3. Although glycerin conversion increased with increase in WGR from 3:1 to 6:1, it was almost constant when the WGR increased from 6:1 to 9:1 for $Rh/CeO_2/Al_2O_3$. Glycerin conversion was almost 90% at WGR 9:1 with Ni/Al_2O_3, whereas it was 93% in case of $Rh/CeO_2/Al_2O_3$. With the increase in WGR, the H_2 selectivity increased with both catalysts. H_2 selectivity of about 80% (5 mols of H_2) was obtained with Ni/Al_2O_3, whereas it was only 71% with $Rh/CeO_2/Al_2O_3$ at WGR 9:1. At the same time, with the increase in WGR from 3:1 to 6:1, the production of CH_4 was completely inhibited in the case of Ni/Al_2O_3, whereas no CH_4 was observed in any WGR with $Rh/CeO_2/Al_2O_3$ at 900 °C and FFR 0.15 ml/min. Similarly, with the increase in WGR, the selectivity towards H_2 and CO_2 were increased. The increase in H_2 and CO_2 selectivity could be attributed to the water gas shift reaction. Increase in WGR also increased the H_2 selectivity and conversion. However, the reforming process consumed a considerable amount of energy with the increase in water molar ratio. For example, the total amount of energy required to carry out the experiment at 900 °C is about 55% of the heating value of glycerin (1485 kJ/mol) with the WGR 9:1. However, the process only requires 28% of the heating value of glycerin if the reaction is conducted at stoichiometric ratio of glycerin and water (i.e., WGR = 3:1) at 900 °C.

3.4. Effect of metal loading

Catalysts with three different metal loadings (3.5, 2.5, and 1.5 wt%) were prepared for Ni/Al_2O_3 and $Rh/CeO_2/Al_2O_3$ to see the effect of the metal percentage on selectivity of H_2 and other gases, and glycerin conversion. In the case of $Rh/CeO_2/Al_2O_3$, the metal loading of Ce was 2.5 wt% for all the catalysts. Fig. 7 shows the effect of the metal loading in terms of selectivity and glycerin conversion. As can be seen from Fig. 7, with the increase in metal loading the glycerin conversion increased for both catalysts. At 1.5 wt%, the glycerin conversion was 75% and increased to 81% with the metal loading of 2.5 wt% in case of Ni/Al_2O_3. Similarly, 90% of glycerin conversion was found with $Rh/CeO_2/Al_2O_3$ at 2.5 wt%, whereas it was 78% conversion at 1.5 wt% under the same conditions. At 3.5 wt% of metal loading, the glycerin conversion was about 94% in both the catalysts. Although glycerin conversion increased with the metal loading, H_2 selectivity did not increase much. H_2 selectivity as well as the selectivity of CO, CH_4, and CO_2 was found to be almost stable at different metal loadings investigated under this study.

3.5. Catalyst durability results

Fig. 8 shows catalyst durability results over Ni/Al_2O_3 and $Rh/CeO_2/Al_2O_3$. As can be seen from the figure, H_2 selectivity and conversion remained almost the same over 13 h of operation over Ni/Al_2O_3. Although the loss of structural rigidity was observed at lower temperatures (Section 3.1), it was not the case at 900 °C. The glycerin conversion was approximately 80% and the H_2 selectivity remained 73–74% under the experimental conditions investigated in this study over Ni/Al_2O_3. In the case of Rh/CeO_2, glycerin conversion remained almost constant over the time period whereas the H_2 selectivity decreased initially and remained constant thereafter.

3.6. XRD and SEM images

Fig. 9 shows scanning electron microscope (SEM) images of blank monoliths (Al_2O_3), Ni/Al_2O_3, Rh/Al_2O_3, CeO_2/Al_2O_3, and $Rh/CeO_2/Al_2O_3$. Comparing Fig. 9(a) and (b), it can be inferred that the small particles seen in Fig. 9(b) are Ni particles. Similarly, comparing Fig. 9(a) and (c), it can be seen that the particles in Figure (c) is more lustrous than Figure (a) and it can be assumed that lustrous particles are due to effect of Rh particles. We could not see much difference between Fig. 9(a) and (d) because CeO_2 phase had a significantly smaller crystalline size than Al_2O_3 phase. Therefore, shining particles in Fig. 9(e) are also Rh metal particles and they might be in CeO_2/Al_2O_3 supports. Looking into the five figures, it can be inferred that the metal particles are homogeneously dispersed. Table 1 depicts the phases present in two samples obtained from XRD analysis. Interestingly, we did not find any rhodium oxide in $Rh/CeO_2/Al_2O_3$. We believe that either rhodium oxides were in the amorphous phase or their size is too small to be detected by XRD. However, less than 10 wt% of the sample was in amorphous in both the catalysts. The weight percentage of

Table 1
XRD analysis for Ni/Al_2O_3 and $Rh/CeO_2/Al_2O_3$

Sample	Phases present	Wt%, ±4%
Ni/Al_2O_3	Al_2O_3	60.5
	$Al_6Si_2O_{13}$	38.2
	NiO	1.3
$Rh/CeO_2/Al_2O_3$	Al_2O_3	57.6
	$Al_6Si_2O_{13}$	38.0
	CeO_2	4.4

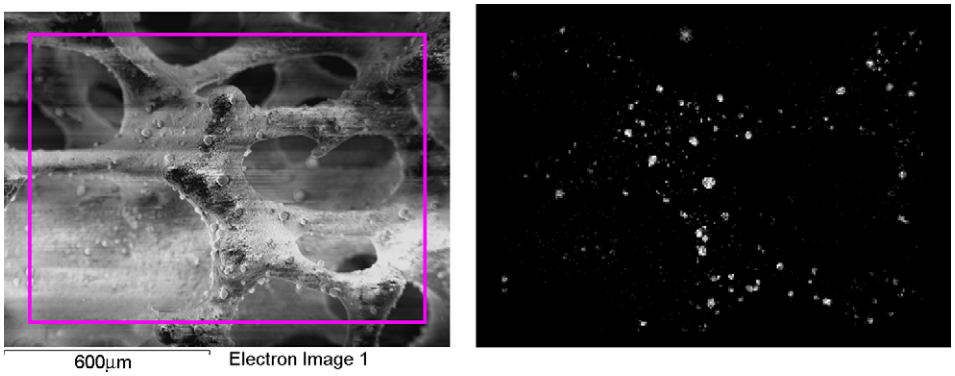

Fig. 10. Energy dispersive spectroscopy (EDS) mapping for Ni/Al_2O_3 (rectangular box in the figure on the left hand side shows the area of the sample used for EDS mapping and the figure on the right hand side shows EDS mapping for Ni).

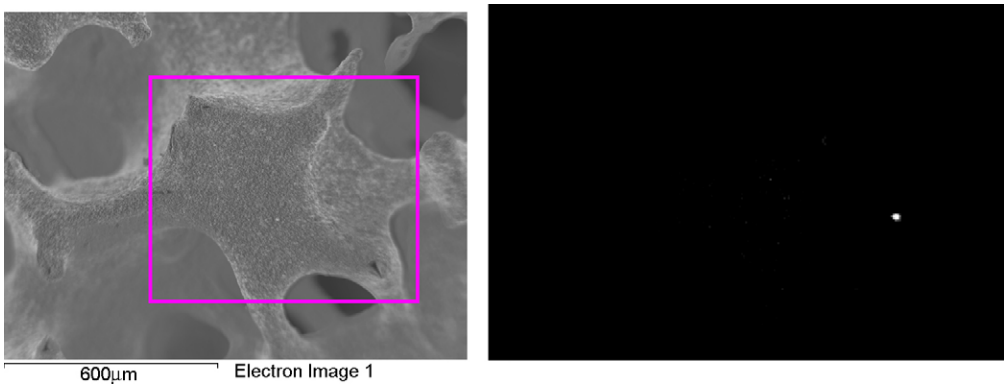

Fig. 11. Energy dispersive spectroscopy (EDS) mapping for $Rh/CeO_2/Al_2O_3$ (rectangular box in the figure on the left hand side shows the area of the sample used for EDS mapping and the figure on the right hand side shows EDS mapping for Rh).

different phases in the sample was calculated by reference intensity ratio (RIR) method. Figs. 10 and 11 show the energy dispersive spectroscopy (EDS) mapping taken from Oxford Instruments for Ni/Al_2O_3 and $Rh/CeO_2/Al_2O_3$ samples, respectively. Ni particles can be clearly seen (Fig. 10); however, Rh particles were not seen distinctly expect one dot (Fig. 11). At this point we are unaware of the exact reason why Rh particles are not observable in CeO_2/Al_2O_3 support.

4. Conclusions

The study on glycerin steam reforming for hydrogen production over Al_2O_3 and CeO_2/Al_2O_3-supported catalysts was performed. Under the reaction conditions investigated, among 14 catalysts, Ni/Al_2O_3 and $Rh/CeO_2/Al_2O_3$ were found to be the best performing catalysts in terms of H_2 selectivity and glycerin conversion. Effects of the glycerin to water molar ratio, feed flow rate, and metal loading were also investigated. It was found that with the increase in the WGR, H_2 selectivity and glycerin conversion increased. About 80% of H_2 selectivity was obtained with Ni/Al_2O_3, whereas it was 71% with $Rh/CeO_2/Al_2O_3$ at WGR 9:1 at 900 °C and FFR 0.15 ml/min. However, H_2 production efficiency could be reduced because of increased enthalpy needs for water evaporation. At low flow rates, for example, 0.15 ml/min, the CH_4 production was completely inhibited in both catalysts, Ni/Al_2O_3 and $Rh/CeO_2/Al_2O_3$. Although increase in metal loading increased glycerin conversion for both catalysts, it was not necessarily the case for H_2 selectivity. At 3.5 wt% of metal loading, glycerin conversion was about 94% in both the catalysts.

References

[1] B.C.R. Ewan, R.W.K. Allen, Int. J. Hydrogen Energy 30 (2005) 809.
[2] Y. Yang, J. Ma, F. Wu, Int. J. Hydrogen Energy 32 (2006) 877.
[3] S. Dunn, Int. J. Hydrogen Energy 27 (2002) 235.
[4] W.E. Bradshaw, C.M. Holzapfel, Science 312 (2006) 1477.
[5] G.A. Deluga, J.R. Salge, L.D. Schmidt, X.E. Verykios, Science 303 (2004) 993.
[6] S. Cavallaro, V. Chiodo, S. Freni, N. Mondello, F. Frusteri, Appl. Catal. A: Gen. 249 (2003) 119.
[7] M. Benito, J.L. Sanz, R. Isabel, R. Padilla, R. Arjona, L. Daza, J. Power Sources 151 (2005) 11.
[8] E.Y. García, M.A. Laborde, Int. J. Hydrogen Energy 16 (1991) 307.
[9] Biofuels for transport: An international perspective. International Energy Agency, Paris, 2004, p. 210.
[10] J.V. Gerpen, Fuel Process. Technol. 86 (2005) 1097.
[11] Available from http://biodiesel.org/resources/faqs/ (Accessed June 21, 2006).
[12] T. Hirai, N.O. Ikenaga, T. Mayake, T. Suzuki, Energy Fuels 19 (2005) 1761.
[13] S. Czernik, R. French, C. Feik, E. Chornet, Ind. Eng. Chem. Res. 41 (2002) 4209.
[14] R.D. Cortright, R.R. Davda, J.A. Dumesic, Nature 418 (2002) 964.
[15] G.W. Huber, J.W. Shabaker, J.A. Dumesic, Science 300 (2003) 2075.

[16] R.R. Davda, J.W. Shabker, G.W. Huber, R.D. Cortright, J.A. Dumesic, Appl. Catal. B: Environ. 56 (2005) 171.
[17] J.W. Shabaker, J.A. Dumesic, Ind. Eng. Chem. Res. 43 (2004) 3105.
[18] A national vision of America's transition to a hydrogen economy to 2030 and beyond. U. S. Department of Energy, Washington DC, 2002, p. 35.
[19] J. Sehested, Catal. Today 111 (2006) 103.
[20] A.N. Fatsikostas, D.I. Kondarides, X.E. Verykios, Chem. Commun. (2001) 851.
[21] F. Mariño, M. Boveri, G. Baronetti, M. Laborde, Int. J. Hydrogen Energy 29 (2004) 67.
[22] A.N. Fatsikostas, X.E. Verykios, J. Catal. 225 (2004) 439.
[23] F. Frusteri, S. Freni, V. Chiodo, G. Bonura, S. Donato, S. Cavallaro, Chem. Eng. Trans. 4 (2004) 117.
[24] F. Mariño, M. Boveri, G. Baronetti, M. Laborde, Int. J. Hydrogen Energy 26 (2001) 665.
[25] H. Idriss, Platinum Met. Rev. 48 (2004) 105.
[26] S. Cavallaro, Energy Fuels 14 (2000) 1195.
[27] A. Haryanto, S. Fernando, N. Murali, S. Adhikari, Energy Fuels 19 (2005) 2098.
[28] P.D. Vaidya, A.E. Rodrigues, Chem. Eng. J. 117 (2006) 39.
[29] D.K. Liguras, D.I. Kondarides, X.E. Verykios, Appl. Catal. B: Environ. 43 (2003) 345.
[30] E.C. Wanat, K. Venkataraman, L.D. Schmidt, Appl. Catal. A: Gen. 276 (2004) 155.
[31] R.R. Soares, D.A. Simonetti, J.A. Dumesic, Angew. Chem. Int. Ed. 45 (2006) 3982.
[32] V. Fierro, V. Klouz, O. Akdim, C. Mirodatos, Catal. Today 75 (2002) 141.
[33] A.N. Fatsikostas, D.I. Kondarides, X.E. Verykios, Catal. Today 75 (2002) 145.
[34] S. Adhikari, S. Fernando, S.R. Gwaltney, S.D.F. To, R.M. Bricka, P.H. Steele, A. Haryanto, Int. J. Hydrogen Energy, in press.
[35] B. Zhang, X. Tang, W. Cai, Y. Xu, W. Shen, Catal. Commun. 7 (2006) 367.